

The Pure Leptonic Decays of B_c Meson and Their Radiative Corrections

Chao-Hsi Chang^{a,b}; Cai-Dian Lü^{b,c}, Guo-Li Wang^b; Hong-Shi Zong^b

^a *CCAST (World Laboratory), P.O. Box 8730, Beijing 100080, China*

^b *Institute of Theoretical Physics, Academia Sinica, P.O. Box 2735, Beijing 100080, China*

^c *Department of Physics, Hiroshima University, 1-3-1 Kagamiyama, 739-8526*

Higashi-Hiroshima, Japan

Abstract

The radiative corrections to the pure leptonic decay $B_c \rightarrow \ell \nu_\ell$ up-to one-loop order is presented. How to cancel the infrared divergences appearing in the loop calculations, and the radiative decay $B_c \rightarrow \ell \nu_\ell \gamma$ is shown precisely. It is emphasized that the radiative decay may be separated properly and may compare with measurements directly as long as the theoretical ‘softness’ of the photon corresponds to the experimental resolutions. Furthermore with a kind of non-relativistic constituent quark model, a kind of typical long distance contributions to the radiative decays is estimated, and it is shown that the contributions are negligible in comparison with the accuracy of one-loop corrections and the expected experimental measurements.

13.30.Ce, 13.40.Ks, 13.38.Lg, 12.39.Jh

I. INTRODUCTION

The pure leptonic decays of the heavy meson B_c are very interesting [1–7]. In principle, the pure-leptonic decay $B_c \rightarrow \ell \nu_\ell$ (see, Fig.1) can be used to determine the decay constant f_{B_c} if the fundamental Cabibbo-Kobayashi-Maskawa matrix element V_{bc} of Standard Model (SM) is known. Conversely if we know the value of decay constant f_{B_c} from other method, these process also can be used to extract the matrix element V_{bc} . The B_c meson has recently been observed at Fermilab [8], that opens a ‘new page’ for the experimental study of B_c meson. Based on the estimates in Refs. [9,10], numerous B_c mesons will be produced in Tevatron and also in LHC. Considering the schedule for the new runs at Tevatron and LHC constructing, we may expect that experimental studies on the B_c meson with more care and much higher statistics will be accessible in the foreseeable future.

The pure leptonic weak decays of the pseudoscalar meson corresponding to Fig.1 are helicity suppressed by factor of $m_\ell^2/m_{B_c}^2$:

$$\Gamma(B_c \rightarrow \ell \bar{\nu}_\ell) = \frac{G_F^2}{8\pi} |V_{bc}|^2 f_{B_c}^2 m_{B_c}^3 \frac{m_\ell^2}{m_{B_c}^2} \left(1 - \frac{m_\ell^2}{m_{B_c}^2}\right)^2, \quad (1)$$

whereas to study them with their radiative decays $B_c \rightarrow l \nu_l \gamma$ simultaneously is attractive [3–5]. Of them only the process $B_c \rightarrow \tau \nu_\tau$ is special i.e. it does not suffer so much from the helicity suppression thus its branching ratio may reach to 1.5% [1] in SM. However the produced τ will decay promptly and one more neutrino is generated in the cascade decay at least, thus it makes the decay channel difficult to be observed, especially, in such a strong background of hadronic collisions.

Fortunately, having an extra real photon emitted in the leptonic decays, the radiative pure leptonic decays can escape from the suppression, furthermore, as pointed out in [3], with the extra photon to identify the produced meson B_c experimentally in hadronic collisions from the backgrounds has advantages, namely in Tevatron and LHC to observe the radiative decays certainly has advantages to compare with the pure leptonic ones. Although the

radiative corrections are suppressed by an extra electromagnetic coupling constant α , it will not be suppressed by the helicity suppression. Therefore, the radiative decay may be comparable, even larger than the corresponding pure leptonic decays. Considering the possibility to measure the decay constant f_{B_c} and the CKM matrix element V_{cb} in LHC in the foreseeable future, the problem to increase the accuracy of the theoretical calculation, at least up to the first order radiative corrections, emerges.

The radiative pure leptonic decays, theoretically, have inferred divergences and will be canceled with those from loop corrections of the pure leptonic decays, thus we are also interested in considering the radiative decays and the pure leptonic decays with one-loop radiative corrections together. Moreover, all of them can be divided into two components: 1). The so-called short distance contributions, for instance, those of the radiative pure leptonic decays correspond to the four diagrams in Fig.2, i.e. a real photon is attached to any of the charged lines of the pure-leptonic decay Feynman diagrams Fig.1.

2). The so-called long distance contributions which are relevant to a virtual heavy hadronic state as an intermediate state. To increase the accuracy of the theoretical calculation, both components should consider precisely.

Recently, there are a few papers [3–5] on the radiative processes with different methods in literature, but inconsistent results have been obtained no matter all of them just the lowest order calculations. To clarify the inconsistency, i.e. further to re-examine the process is certainly needed. Furthermore, since in Ref. [4] an approach of QCD sum rule is adopted and in Ref. [3] a kind of quark model is adopted, QCD sum rule is supposed some long distance effects may be taken into account, so it is reasonable to doubt that the disagreement between the results of Refs. [3,4] could be due to the long distance contributions. We essentially will adopt the same approach as Ref. [3], thus in the paper we especially make some estimates on the long distance contributions precisely.

Namely in the present paper, baring the problems and the situation pointed out above in mind, we will investigate the B_c leptonic decays up-to one loop radiative corrections carefully.

The paper is organized as follow: in Section II, we present the calculations of all the short distance contributions: *i*) besides the leptonic decays shown as Fig.1, the radiative decays into three family leptons with a real photon appearing in the final state as shown in Fig.2; *ii*) the virtual photon corrections to the pure leptonic decays i.e. a photon in loop as shown in Figs.3.1, 3.2, 3.3, 3.4. In Section III, we estimate a typical contributions from the long distance contributions. In Sec.IV, we evaluate the values of the decays. As uncertainties the dependence of the results on the parameters appearing in the considered model is discussed. Comparison with the others' results are made. Finally, preliminary conclusion is obtained.

II. THE SHORT DISTANCE CONTRIBUTIONS

Let us start with the radiative decay. The short distance contributions are corresponding to the four diagrams in Fig.2. According to the constituent quark model which is formulated by Bethe-Salpeter (B.-S.) equation, the amplitude turns out to be the four terms $M_i(i = 1, 2, 3, 4)$:

$$M_1 = Tr \left[\int \frac{d^4 q}{(2\pi)^4} \chi(p, q) i \left(\frac{G_F m_w^2}{\sqrt{2}} \right)^{\frac{1}{2}} \gamma_\mu (1 - \gamma_5) V_{bc} \right] \times \\ \frac{i \left(-g^{\mu\nu} + \frac{p^\mu p^\nu}{m_w^2} \right)}{p^2 - m_w^2} ie [(p' + p)_\lambda g_{\nu\rho} + (k - p')_\nu g_{\rho\lambda} + (-p - k)_\rho g_{\nu\lambda}] \epsilon^\lambda \times \\ \frac{i \left(-g^{\rho\sigma} + \frac{(p-k)^\rho (p-k)^\sigma}{m_w^2} \right)}{(p - k)^2 - m_w^2} \bar{\ell} \frac{ig}{2\sqrt{2}} \gamma_\sigma (1 - \gamma_5) \nu_\ell, \quad (2)$$

$$M_2 = Tr \left[\int \frac{d^4 q}{(2\pi)^4} \chi(p, q) i \left(\frac{G_F m_w^2}{\sqrt{2}} \right)^{\frac{1}{2}} \gamma_\mu (1 - \gamma_5) V_{bc} \right] \frac{i \left(-g^{\mu\nu} + \frac{p^\mu p^\nu}{m_w^2} \right)}{p^2 - m_w^2} \\ \times \bar{\ell} (-ie) \not{k}_\ell \frac{i}{\not{k}_\ell - m_\ell} \frac{ig}{2\sqrt{2}} \gamma_\nu (1 - \gamma_5) \nu_\ell, \quad (3)$$

$$M_3 = Tr \left[\int \frac{d^4 q}{(2\pi)^4} \chi(p, q) i \left(\frac{G_F m_w^2}{\sqrt{2}} \right)^{\frac{1}{2}} \gamma_\mu (1 - \gamma_5) V_{bc} \frac{i}{\frac{m_b}{m_b + m_c} \not{p} + \not{q} - \not{k} - m_b} \left(-i \frac{e}{3} \not{\ell} \right) \right]$$

$$\times \frac{i \left(-g^{\mu\sigma} + \frac{(p-k)^\mu(p-k)^\sigma}{m_w^2} \right)}{(p-k)^2 - m_w^2} \bar{\ell} \frac{ig}{2\sqrt{2}} \gamma_\sigma (1 - \gamma_5) \nu_\ell, \quad (4)$$

$$M_4 = Tr \left[\int \frac{d^4 q}{(2\pi)^4} \chi(p, q) \left(i \frac{2e}{3} \not{\epsilon} \right) \frac{i}{-(\frac{m_c}{m_b+m_c} \not{p} + \not{q} - \not{k}) - m_c} i \left(\frac{G_F m_w^2}{\sqrt{2}} \right)^{\frac{1}{2}} \gamma_\mu (1 - \gamma_5) V_{bc} \right] \\ \times \frac{i \left(-g^{\mu\sigma} + \frac{(p-k)^\mu(p-k)^\sigma}{m_w^2} \right)}{(p-k)^2 - m_w^2} \bar{\ell} \frac{ig}{2\sqrt{2}} \gamma_\sigma (1 - \gamma_5) \nu_\ell, \quad (5)$$

where $\chi(p, q)$ is Bethe-Salpeter wave function of the meson B_c ; p is the momentum of B_c ; ϵ, k are the polarization vector and momentum of the emitted photon. In the quark model, the momenta of \bar{b}, c -quarks inside the bound state i.e. the B_c meson, are:

$$p_b = \frac{m_b}{m_b + m_c} p + q; \quad p_c = \frac{m_c}{m_b + m_c} p - q,$$

where q is the relative momentum of the two quarks inside the B_c meson. As the B_c meson is a nonrelativistic bound state in nature, so the higher order relativistic corrections may be computed precisely, but being an approximation for a S -wave state, and focusing the light on the radiative decay corrections only at this moment now, we ignore q dependence i.e. we may still have the non-relativistic spin structure for the wave function of the meson B_c (a 1S_0 state) correspondingly:

$$\int \frac{d^4 q}{(2\pi)^4} \chi(p, q) = \frac{\gamma_5(\not{p} + m)}{2\sqrt{m}} \psi(0).$$

Here $\psi(0)$ is the wave function at origin, and by definitions it connects to the decay constant f_{B_c} :

$$f_{B_c} = \frac{\psi(0)}{2\sqrt{m}},$$

where m is the mass of B_c meson. Moreover we note that for convenience we take unitary gauge for weak bosons to do the calculations throughout the paper. With a straightforward computation, the amplitude can be simplified as:

$$M_1 = \frac{-4Ai}{(m^2 - m_w^2)(m^2 - 2p \cdot k - m_w^2)} \times$$

$$\bar{\ell} \left(-1 + \frac{m^2}{m_w^2} \right) \left[p \cdot \epsilon(k - p) - (2p \cdot k - m^2) \not{e} \right] (1 - \gamma_5) \nu_\ell, \quad (6)$$

$$M_2 = \frac{4Ai}{(m^2 - m_w^2)(2k_1 \cdot k)} \bar{\ell} \left(-1 + \frac{m^2}{m_w^2} \right) \not{e}(k_1 + \not{k} + m_e) \not{p} (1 - \gamma_5) \nu_\ell, \quad (7)$$

$$\begin{aligned} M_3 + M_4 = & \frac{-4Ai}{(-p \cdot k)(m^2 - 2p \cdot k - m_w^2)} \bar{\ell} \left\{ [-(p \cdot \epsilon) \not{p} + (p \cdot \epsilon) \not{k} - p \cdot k \not{e}] s_2 \right. \\ & \left. + is_1 \epsilon^{\alpha\mu\beta\nu} p_\alpha \epsilon_\mu k_\beta \gamma_\nu \right] + \frac{(p \cdot k)}{m_w^2} p \cdot \epsilon (m^2 - p \cdot k) \} (1 - \gamma_5) \nu_\ell, \end{aligned} \quad (8)$$

where k_1 is the momentum of the charged lepton, and

$$\begin{aligned} A &= \frac{\psi(0) \left(\frac{G_F m_w^2}{\sqrt{2}} \right)^{\frac{1}{2}} V_{bc} e g}{2\sqrt{m} 2\sqrt{2}} = \frac{\psi(0) \left(\frac{G_F m_w^2}{\sqrt{2}} \right) V_{bc} e}{2\sqrt{m}}; \\ s1 &= -\frac{m_b + m_c}{6m_b} + \frac{m_b + m_c}{3m_c}; \quad s2 = \frac{m_b + m_c}{6m_b} + \frac{m_b + m_c}{3m_c}. \end{aligned}$$

As a matter of fact, there is infrared infinity when performing phase space integral about the square of matrix element at the soft photon limit. It is known that the infrared infinity can be cancelled completely by that of the loop corrections to the corresponding pure leptonic decay $B_c \rightarrow l\nu$.

In Eqs.(7) and (8), the infrared terms can be read out:

$$M^i = M_2^i + M_3^i + M_4^i = \frac{4Ai}{m_w^2} \bar{\ell} \left[\frac{k_1 \cdot \epsilon \not{p}}{k_1 \cdot k} - \frac{p \cdot \epsilon \not{p}}{p \cdot k} \right] (1 - \gamma_5) \nu_\ell. \quad (9)$$

As the diagrams (g), (h), (i), (j) in Figs.3.3, 3.4 always have a further suppression factor m^2/m_w^2 to compare with the other loop diagrams, we may ignore the contributions from these four diagrams savey. Furthermore we should note that in our calculations throughout the paper, the dimensional regularization to regularize both infrared and ultraviolet divergences is adopted, while the on-mass-shell renormalization for the ultraviolet divergence is used.

If Feynman gauge for photon is taken (we always do so in the paper), the amplitude corresponding to the diagrams (a), (b) of Fig.3.1 can be written as:

$$M_{(2)}(a) = \frac{2}{3}eA \int \frac{d^4l}{(2\pi)^4} \left[\frac{-4i\varepsilon^{\alpha\mu\beta\nu}p_\alpha l_\beta - 4(p_\mu l_\nu - p \cdot l g_{\mu\nu} + p_\nu l_\mu) + \frac{8m_c}{m_b+m_c}p_\mu p_\nu}{l^2(l^2 - 2p \cdot l - m_w^2)(l^2 - \frac{2m_c}{m_b+m_c}p \cdot l)[l^2 - 2l \cdot (p - k_2)]} \right] \times \bar{\ell}[2(p - k_2)_\mu - \gamma_\mu]\ell(-\gamma_\nu)(1 - \gamma_5)\nu_\ell, \quad (10)$$

$$M_{(2)}(b) = -\frac{1}{3}eA \int \frac{d^4l}{(2\pi)^4} \left[\frac{-4i\varepsilon^{\alpha\mu\beta\nu}p_\alpha l_\beta + 4(p_\mu l_\nu - p \cdot l g_{\mu\nu} + p_\nu l_\mu) - \frac{8m_b}{m_b+m_c}p_\mu p_\nu}{l^2(l^2 - 2p \cdot l - m_w^2)(l^2 - \frac{2m_b}{m_b+m_c}p \cdot l)[l^2 - 2l \cdot (p - k_2)]} \right] \times \bar{\ell}[2(p - k_2)_\mu - \gamma_\mu]\ell(-\gamma_\nu)(1 - \gamma_5)\nu_\ell, \quad (11)$$

where the l , k_2 denote the momenta of the loop and the neutrino respectively. These two terms also have infrared infinity when integrating out the loop momentum l .

After doing the on-mass-shell subtraction, the terms corresponding to vertex and self-energy diagrams (c), (d), (e), (f) can be written as:

$$\begin{aligned} M_{(2)}(c+d+e+f) &= \frac{ieA}{4\pi^2}\bar{\ell}\not{p}(1-\gamma_5)\nu_\ell \times \left[\ln(4) - \frac{8}{9} + \frac{2}{9}\frac{m_b-m_c}{m_b+m_c}\ln\left(\frac{m_b}{m_c}\right) \right. \\ &\quad + \left(\frac{2}{9} + \frac{8}{9}\frac{m_c}{m_b+m_c} \right) \ln\left(\frac{m_b+m_c}{m_b}\right) + \left(\frac{8}{9} + \frac{8}{9}\frac{m_c}{m_b+m_c} \right) \ln\left(\frac{m_b+m_c}{m_c}\right) \\ &\quad \left. + \frac{2}{\varepsilon_I} - 2\gamma + \ln\left(\frac{4\pi\mu^2}{m^2}\right) + \ln\left(\frac{4\pi\mu^2}{m_e^2}\right) \right]. \end{aligned} \quad (12)$$

Now let us see the cancellation of the infrared divergencies precisely. The infrared parts of the decay widths which are from the interference of the self-energy and vertex correction diagrams with the tree diagrams:

$$\begin{aligned} \delta\Gamma_{s,v}^{infrared} &= \left(\frac{\alpha V_{bc}^2 f_{B_c}^2 G_F^2 M m_\ell^2}{16\pi^2} \right) \left[-\frac{34}{9} - \frac{4}{9}\frac{m_b-m_c}{m_b+m_c}\ln\left(\frac{m_b}{m_c}\right) \right. \\ &\quad - \left(\frac{2}{9} + \frac{4}{9}\frac{m_c}{m_b+m_c} \right) \ln\left(\frac{m_b+m_c}{m_b}\right) - \left(-\frac{4}{9} + \frac{4}{9}\frac{m_b}{m_b+m_c} \right) \ln\left(\frac{m_b+m_c}{m_c}\right) \\ &\quad \left. - \frac{2}{\varepsilon_I} + 2\gamma - \ln\left(\frac{4\pi\mu^2}{m^2}\right) - \ln\left(\frac{4\pi\mu^2}{m_e^2}\right) \right]; \end{aligned} \quad (13)$$

the infrared part of the decay widths from the interference of the "box" correction diagrams with the tree diagrams:

$$\delta\Gamma_{box}^{infrared} = \left(\frac{\alpha V_{bc}^2 f_{B_c}^2 G_F^2 M m_\ell^2}{16\pi^2} \right) \left[- \left(\frac{1}{\varepsilon_I} - \gamma \right) \ln \left(\frac{m_\ell^2}{M^2} \right) - \ln \left(\frac{m_\ell^2}{M^2} \right) \ln \left(\frac{4\pi\mu^2}{M^2} \right) \right]; \quad (14)$$

the infrared part of the decay width from the real photon emission:

$$\begin{aligned} \delta\Gamma_{real}^{infrared} &= \left(\frac{\alpha V_{bc}^2 f_{B_c}^2 G_F^2 M m_\ell^2}{16\pi^2} \right) \\ &\cdot \left[\frac{2}{\varepsilon_I} - 2\gamma + \left(\frac{1}{\varepsilon_I} - \gamma \right) \ln \left(\frac{m_\ell^2}{M^2} \right) + \left(2 + \ln \left(\frac{m_\ell^2}{M^2} \right) \right) \ln \left(\frac{4\pi\mu^2}{4(\Delta E)^2} \right) \right]. \end{aligned} \quad (15)$$

Here ΔE is a small energy, which corresponds to the experimental resolution of a soft photon so that the phase space of the emitting photon in fact is divided into a soft and a hard part by ΔE . Where μ is the dimensional parameter appearing in the dimensional regularization. It is easy to check that when adding up all the parts: the real photon emission $\delta\Gamma_{real}^{infrared}$ and the virtual photon corrections $\delta\Gamma_{s,v}^{infrared}, \delta\Gamma_{box}^{infrared}$, the infrared divergences $\frac{2}{\varepsilon_I} - \gamma$ are canceled totally and the μ dependence is also cancelled. Hence we may be sure that we finally obtain the pure leptonic widths for the B_c meson decays to the three families of leptons which are accurate up-to the ‘next’-order corrections and ‘infrared finite’ but depend on the experimental resolution ΔE .

III. ESTIMATE OF THE LONG DISTANCE CONTRIBUTIONS

We have done the calculations of the radiative ‘short distance’ corrections corresponding to the energy scale around m_{B_c} , whereas, there are corrections which correspond to much softer nature than what we have considered. Typically, some of them in the radiative decay $B_c \rightarrow l\nu\gamma$ may be described by Fig.4. People, generally, call the soft corrections as the ‘long distance contributions’ correspondingly.

To have a rough estimate on the contributions of the softer part and to be typical, let us only consider those corresponding to Fig.4.

The amplitude for the long distance radiative corrections corresponding to Fig.4 may be written as:

$$M = \frac{-ie(2\pi)^4 \delta^4(P_{B_c} - k - k_1 - k_\nu) G_F \epsilon_\mu(k)}{\sqrt{2}} \bar{\ell}(k_1) \gamma^\lambda (1 - \gamma_5) \nu_e(k_\nu)$$

$$\cdot \left[\sum_{\vec{p}_n = \vec{k}} \frac{\langle 0 | j^{\mu em}(0) | p_n \rangle \langle p_n | j_{q\lambda}^+(0) | P_{B_c} \rangle}{2p_{n0}(k_0 - p_{n0} + i\epsilon)} + \sum_{\vec{p}_n = \vec{P}_{B_c} - \vec{k}} \frac{\langle 0 | j_{q\lambda}^+(0) | p_n \rangle \langle p_n | j^{\mu em}(0) | P_{B_c} \rangle}{2p_{n0}(P_{B_{c0}} - k_0 - p_{n0} + i\epsilon)} \right], \quad (16)$$

where $j^{\mu em}$, $j_{q\lambda}^+$ are electromagnetic current and weak current respectively, and $\epsilon(k)$ is polarization vector of the real photon. The intermediate states $|p_n\rangle$ are all the possible physical states, and in the summation $\vec{p}_n = \vec{k}$ for the first term and $\vec{p}_n = \vec{P}_{B_c} - \vec{k}$ for the second term are kept. Note that for the time-component, generally, $k_0 \neq p_{n0}$ for the first term and $p_{n0} \neq P_{B_{c0}} - k_0$ for the second term. To compute the whole amplitude, let us compute the current matrix elements appearing in Eq.(16) with the intermediate meson states being on mass-shell. However to have a rough estimate instead of a precise one, here only the intermediate meson states J/ψ and B_c^* , being of typical long distance contributions, are computed by means of the three Feynman diagrams shown in Fig.4.

According to Eq.(16), we have:

$$\langle 0 | j^{\mu em}(0) | p_{J/\psi} \rangle = -\frac{2}{3} \frac{1}{\sqrt{2\pi p_{J/\psi 0}}} \phi_{J/\psi}(0) M_{J/\psi} \epsilon_\mu(J/\psi), \quad (17)$$

$$\langle 0 | j_{q\lambda}^+(0) | p_{B_c^*} \rangle = -\frac{1}{\sqrt{2\pi p_{B_{c0}^*}}} \phi_{B_c^*}(0) M_{B_c^*} \epsilon_\mu(B_c^*). \quad (18)$$

The matrix element $\langle p_{J/\psi} | j_{q\lambda}^+(0) | P_{B_c} \rangle$ can be decomposed into two parts:

$$\langle p_{J/\psi} | j_{q\lambda}^+(0) | P_{B_c} \rangle = \langle p_{J/\psi} | V_\lambda | P_{B_c} \rangle - \langle p_{J/\psi} | A_\lambda | P_{B_c} \rangle, \quad (19)$$

namely those of the vector current $V_\lambda = \frac{1}{2}\bar{c}\gamma_\lambda b$ and the axial current $A_\lambda = \frac{1}{2}\bar{c}\gamma_\lambda\gamma_5 b$. They are related to the form factors [1,11,12] as follows:

$$\langle p_{J/\psi} | V_\mu | P_{B_c} \rangle = ig \frac{1}{2} \varepsilon_{\mu\nu\rho\sigma} \epsilon^{*\nu} (P_{B_c} + p_{J/\psi})^\rho (P_{B_c} - p_{J/\psi})^\sigma, \quad (20)$$

$$\langle p_{J/\psi} | A_\mu | P_{B_c} \rangle = \frac{1}{2} [f \epsilon_\mu^* + a_+ (\epsilon^* \cdot P_{B_c}) (P_{B_c} + p_{J/\psi})_\mu + a_- (\epsilon^* \cdot P_{B_c}) (P_{B_c} - p_{J/\psi})_\mu], \quad (21)$$

where g, f, a_+, a_- are the possible form factors. For convenience, here we actually calculate the matrix element $\langle p_{B_c} | j^{\mu em}(0) | P_{B_c^*} \rangle$ instead of $\langle p_{B_c^*} | j^{\mu em}(0) | P_{B_c} \rangle$:

$$\langle p_{B_c} | j^{\mu em}(0) | P_{B_c^*} \rangle = i(c_b g_b + c_c g_c) \epsilon_{\mu\nu\rho\sigma} \epsilon^{*\nu}(B_c^*) (P_{B_c^*} + p_{B_c})^\rho (P_{B_c^*} - p_{B_c})^\sigma \quad (22)$$

Now we just present the final results of the form factors g, f, a_+, a_-, g_b, g_c here, as the detail calculations on them can be found in Ref.[1].

Let us introduce further definitions, which is convenient for presenting the results. If p_1, p_2 are the momenta of the constituent particles 1 and 2 respectively, the total and the relative momenta p and q are defined as:

$$p_1 = \alpha_1 p + q, \quad \alpha_1 = \frac{m_1}{m_1 + m_2};$$

$$p_2 = \alpha_2 p + q, \quad \alpha_2 = \frac{m_2}{m_1 + m_2}.$$

The momenta p, p' are replaced to denote those for the initial and final mesons $P_{B_c}, p_{B_c^*}$ (or $p_{J/\psi}$), and M, M' are denoted the masses of the initial and final mesons.

Furthermore q_p, q_{pT} are denoted the two Lorentz covariant variables as follows:

$$q_p = \frac{p \cdot q}{M_p}, \quad q_{pT} = \sqrt{q_p^2 - q^2}$$

and:

$$\omega_{ip} = \sqrt{m_i^2 + q_{pT}^2}$$

$$\omega'_{ip'} = \sqrt{m'^2_i + q'_{p'T}^2}.$$

Now we can give the formulas of form factor using the above covariant variables:

$$g = \xi \frac{\omega'_1 + \omega'_2}{MM'm'_1}$$

$$f = \xi \left[\frac{(p \cdot p'_1)}{Mm'_1} + 1 \right]$$

$$a_\pm = \xi \left\{ \frac{2m_2}{M^2m'_1} + \delta \mp \left[\frac{\omega'_1 + \omega'_2}{MM'm'_1} + \frac{(p \cdot p')}{M'^2}\delta \right] \right\} \quad (23)$$

where

$$\delta = -\frac{C[1 + (p \cdot p'_1)/Mm'_1]}{p^2 - (p \cdot p')^2/M'^2}$$

$$C = \frac{1}{L_+ \left[\frac{(p' \cdot p_1)(p' \cdot p'_1)}{M'^2} - \frac{1}{L_-^2} \right]^{1/2} - 1}$$

where

$$L_{\pm} = \left[\frac{1}{2} (p_1 \cdot p'_1 \pm m_1 m'_1) \right]^{-1/2}.$$

The common factor:

$$\xi = \left[\frac{2\omega'_2 m_1^2 m'^2_1}{[(p_1 \cdot p'_1) + m_1 m'_1] \omega_1 \omega'_1 \omega_2} \right]^{1/2} \times \int \frac{d^3 \vec{q}}{(2\pi)^3} \phi'^*_p(q'_{p'_T}) \cdot \phi_p(|\vec{q}|) \quad (24)$$

if it is written in c.m.s. of the initial meson ($\vec{p} = 0$).

Here $\phi'^*_p(q'_{p'_T})$ and $\phi_p(|\vec{q}|)$ [14] correspond to the radius wave functions of the mesons in the initial and final states respectively, but both are presented in c.m.s. of the initial meson. The equations about g_a, g_b are similar as g , we will not repeat them here.

IV. NUMERICAL RESULTS AND DISCUSSION

First of all, let us show the ‘whole’ leptonic decay widths i.e. the sum of the corresponding radiative decay widths and the corresponding pure leptonic decay widths with radiative corrections, and put them in Table (1). As firstly we would like to see the facts of ‘short distance’ contributions, so here only the ‘short distance’ contributions are taken into account. Why we put the radiative decay and the pure leptonic decay with radiative corrections together here is to make the width not to depend on the experimental resolution for a soft photon at all. To compare with the earlier computations [3–5] in the numerical evaluation, the values for the parameters $\alpha = 1/132$ and $|V_{bc}| = 0.04$ [13] are taken, and two possible values for the rests are selected as bellow:

- (1) $m_{B_c} = 6.258$ GeV, $m_b = 4.758$ GeV, $m_c = 1.500$ GeV, $f_{B_c} = 0.360$ GeV [3];
- (2) $m_{B_c} = 6.258$ GeV, $m_b = 4.700$ GeV, $m_c = 1.400$ GeV, $f_{B_c} = 0.350$ GeV [4,5].

Table (1) The ‘Whole’ Leptonic Decay Widths (in unit GeV)

(short distance contributions only)

	(1)	(2)
$\Gamma_e(10^{-17})$	6.444	6.902
$\Gamma_\mu(10^{-16})$	1.383	1.389
$\Gamma_\tau(10^{-14})$	1.871	1.782

For comparison, the width of each pure leptonic decay at tree level with the same parameters as those in Table (1) is put in Table (2).

Table (2) The Pure Leptonic Decay Widths (in unit GeV) of Tree Level

	(1)	(2)
$\Gamma_e(10^{-21})$	1.827	1.727
$\Gamma_\mu(10^{-16})$	0.7841	0.7412
$\Gamma_\tau(10^{-14})$	1.862	1.773

If the lifetime of B_c meson is (a). $\tau(B_c) = 0.46 \times 10^{-12}s$ as indicated by the first observation [8]; (b). $\tau(B_c) = 0.52 \times 10^{-12}s$ as adopted in Ref. [3], the corresponding branching ratios are showed in Tables (3), (4).

Table (3) Branching Ratios of the ‘Whole’ Leptonic Decays
(short distance contributions)

	(1-a)	(2-a)	(1-b)	(2-b)
$B_e(10^{-5})$	5.09	5.45	4.5	4.82
$B_\mu(10^{-5})$	10.93	10.98	9.69	9.76
$B_\tau(10^{-2})$	1.477	1.407	1.306	1.246

Table (4) Tree Level Branching Ratios of The Pure Leptonic Decays

	(1-a)	(2-a)	(1-b)	(2-b)
$B_e(10^{-9})$	1.44	1.36	1.28	1.21
$B_\mu(10^{-4})$	0.62	0.586	0.55	0.52
$B_\tau(10^{-2})$	1.47	1.40	1.30	1.24

To see the contributions of the radiative decays precisely we present the radiative decay widths with a cut of the photon energy i.e. the widths of the radiative decays $B_c \rightarrow l\nu\gamma$ with the photon energy $E_\gamma \geq k_{min}$ as the follows: $k_{min} = 0.1$ GeV, $k_{min} = 0.2$ GeV, $k_{min} = 0.5$ GeV and $k_{min} = 1.0$ GeV respectively in Table (5).

Table (5): The Radiative Decay Widths (in unit 10^{-17} GeV)
(with cuts of the photon momentum and the angle between photon and lepton)

		(1)			(2)		
$k_{min}(GeV)$		5^0	15^0	30^0	5^0	15^0	30^0
0.1	Γ_e	6.384	6.370	6.297	6.832	6.819	6.752
0.2	Γ_e	6.317	6.303	6.242	6.762	6.750	6.693
0.5	Γ_e	5.931	5.918	5.883	6.351	6.340	6.307
1.0	Γ_e	4.807	4.800	4.790	5.151	5.143	5.136
0.1	Γ_μ	6.613	6.518	6.385	7.049	6.958	6.834
0.2	Γ_μ	6.484	6.412	6.306	6.920	6.850	6.753
0.5	Γ_μ	6.018	5.977	5.917	6.433	6.394	6.340
1.0	Γ_μ	4.843	4.824	4.802	5.184	5.165	5.146
0.1	Γ_τ	13.75	13.66	12.88	13.60	13.52	12.78
0.2	Γ_τ	10.87	10.82	10.34	10.86	10.81	10.36
0.5	Γ_τ	7.139	7.121	6.970	7.282	7.265	7.122
1.0	Γ_τ	4.169	4.165	4.146	4.340	4.335	4.318

For the convenience to compare with experiments, we present the photon spectrum of the radiative decays in Fig.6 and give the decay widths of the so-called physical pure leptonic decays: $\Gamma_{phys} = \Gamma_{whole} - \Gamma_{cut}$ where Γ_{cut} are showed in Table (5); Γ_{whole} are showed in Table (1). We put the values of Γ_{phys} in Table (6).

Table (6): Decay widths of Γ_{phys} (10^{-17} GeV)

		(1)			(2)		
$k_{min}(\text{GeV})$		5 ⁰	15 ⁰	30 ⁰	5 ⁰	15 ⁰	30 ⁰
0.1	Γ_e	0.060	0.074	0.147	0.070	0.083	0.150
0.2	Γ_e	0.127	0.141	0.202	0.140	0.152	0.209
0.5	Γ_e	0.513	0.526	0.561	0.551	0.562	0.595
1.0	Γ_e	1.637	1.644	1.654	1.751	1.759	1.766
0.1	Γ_μ	7.217	7.312	7.445	6.837	6.928	7.052
0.2	Γ_μ	7.346	7.418	7.524	6.966	7.036	7.133
0.5	Γ_μ	7.812	7.853	7.913	7.453	7.492	7.546
1.0	Γ_μ	8.987	9.006	9.028	8.702	8.721	8.740
0.1	$\Gamma_\tau(10^3)$	1.857	1.857	1.858	1.768	1.768	1.769
0.2	$\Gamma_\tau(10^3)$	1.860	1.860	1.860	1.771	1.771	1.772
0.5	$\Gamma_\tau(10^3)$	1.864	1.864	1.864	1.775	1.775	1.775
1.0	$\Gamma_\tau(10^3)$	1.866	1.866	1.867	1.777	1.777	1.778

Let us select the parameters as in Ref. [3]: $m_{B_c} = 6.258 \text{ GeV}$, $m_b = 4.758 \text{ GeV}$, $m_c = 1.500 \text{ GeV}$, $f_{B_c} = 0.360 \text{ GeV}$, so as to compare with the short distance contributions and to show the contributions from the typical long distance component concerned in the paper. For each of the family, the contribution to the width:

$$\delta\Gamma_e = 1.828 \times 10^{-18} \text{ GeV},$$

$$\delta\Gamma_\mu = 1.827 \times 10^{-18} \text{ GeV},$$

$$\delta\Gamma_\tau = 1.190 \times 10^{-18} \text{ GeV}.$$

From Table (5), we may see that the present results confirm those in Ref. [3], and the slight differences are mainly due to the radiative corrections and the fact that instead of ignoring in Ref. [3], we keep the lepton mass precisely in the numerical evaluation. In comparison with the short contributions, for the radiative leptonic decays of the B_c meson the long distance contributions $\delta\Gamma_l$, ($l = e, \mu, \tau$) are quite small. It may be the reason that the b and

c quark in B_c meson are heavy. Their heavy mass causes the long distance contributions small. Therefore, it seems that we can conclude that the disagreement between Ref. [3] and Refs. [4,5] is not due to the long distance effects.

In addition, we should note that the widths are quite sensitive to the decay constant f_{B_c} , and the values of the quark masses m_b and m_c .

Note that when we almost completed this paper, one similar paper [15] appeared and its results supported those in Ref. [3] that is in agreement with this paper.

Acknowledgement This work was supported in part by the National Natural Science Foundation of China and the Grant No. LWLZ-1298 of the Chinese Academy of Sciences. One of the author (C.-D. Lü) would also like to thank JSPS for supporting him in research.

REFERENCES

- [1] C.-H. Chang and Y.-Q. Chen, Phys. Rev. D**49** (1994) 3399.
- [2] D.-S. Du, H.-Y. Jin and Y.-D. Yang, preprint BIHEP-Th/97-007, **hep-ph/9705261**.
- [3] C.-H. Chang, J-P Cheng and C-D Lü, Phys. Letts. B**425** (1998) 166, **hep-ph/9712325**.
- [4] T.M. Aliev, M.Savci, Phys. Letts. B**434** (1998) 358, **hep-ph/9804407**.
- [5] T.M. Aliev, M.Savci, **hep-ph/9809555**.
- [6] C.-C. Lih, C.-Q. Geng, W.-M. Zhang, Phys. Rev. D**59** (1999) 114002.
- [7] G. Chiladze, A.F. Falk, A.A. Petrov, JHU-TIPAC-98011, **hep-ph/9811405**.
- [8] F.Abe et al., The CDF Collaboration, Phys. Rev. D**58** (1998) 112004, **hep-ex/9804014**.
- [9] C.-H. Chang and Y.-Q. Chen, Phys. Rev. D**48** (1993) 4086; C.-H. Chang, Y.-Q. Chen, G.-P. Han and H.-T.Jiang, Phys. Lett. B**364** (1995) 78; C.-H. Chang, Y.-Q. Chen, and R.J.Oakes, Phys. Rev. D**54** (1996) 4344.
- [10] K. Cheung, Phys. Rev. Lett. **71** (1993) 3413.
- [11] B. Grinstein, M.B. Wise, and N. Isgur, Phys. Rev. Lett. **56** (1986) 298; N. Isgur, D. Scora, B. Grinstein, and M.B. Wise, Phys. Rev. D**39** (1989) 799.
- [12] T. Altomari and L. Wolfenstein, Phys. Rev. Lett. **58** (1987) 1563; Phys. Rev. D**37** (1988) 681.
- [13] Particle Data Group, Phys. Rev. D**54** Part II (1996) 1.
- [14] C.-H. Chang and Hong-Shi Zong, et al. unpublished.
- [15] P. Colangelo and F. De Fazio, **hep-ph/9904363**.

FIGURES

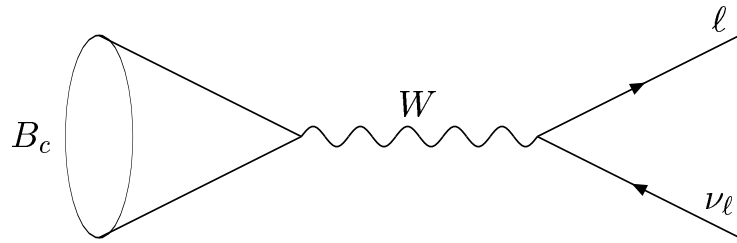


FIG. 1. Tree diagram for $B_c \rightarrow \ell \nu_\ell$.

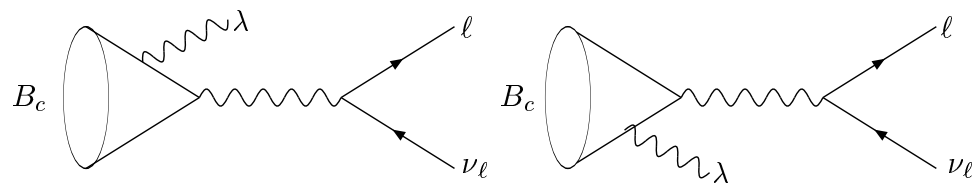
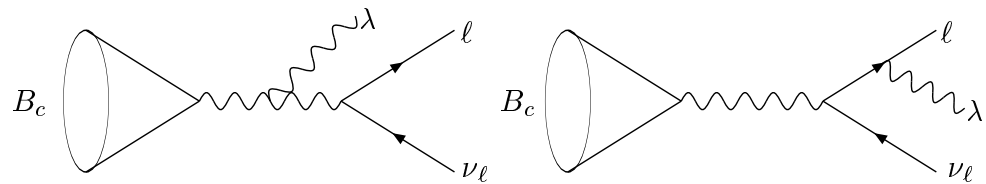


FIG. 2. Diagrams for $B_c \rightarrow \ell \nu \gamma$.

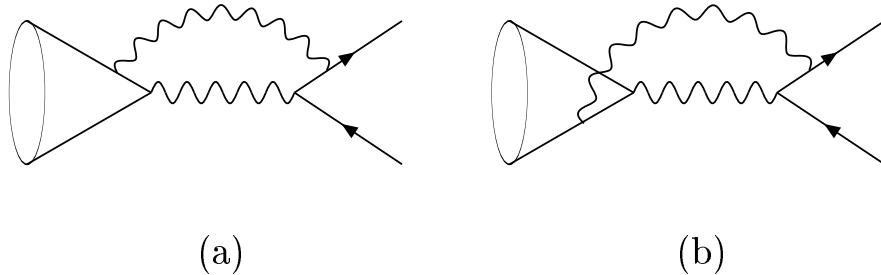
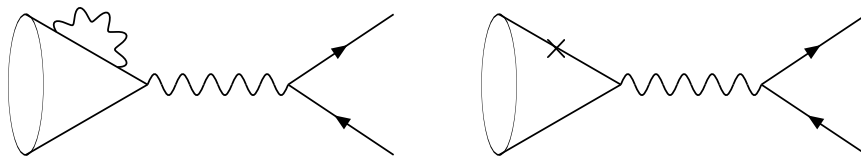
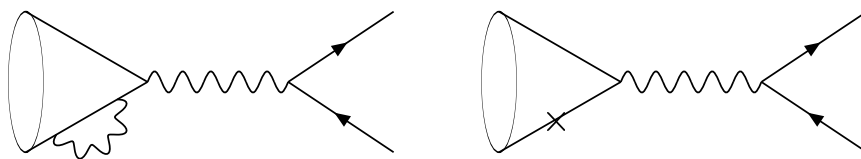


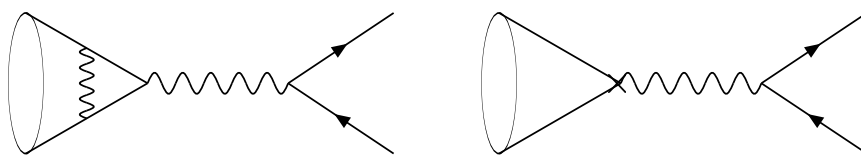
FIG. 3. 1. Box-loop diagrams for $B_c \rightarrow \ell \nu$.



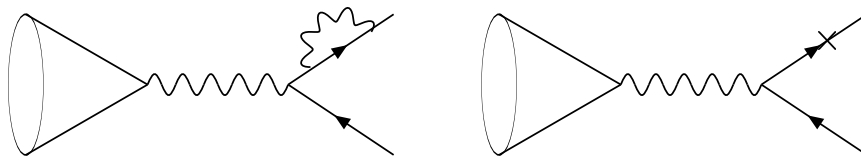
(c)



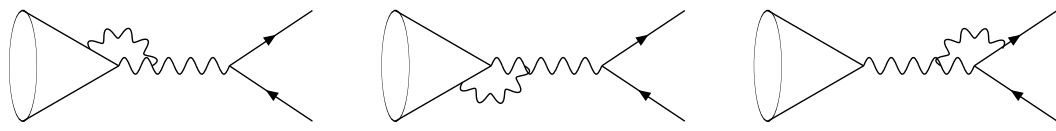
(d)



(e)



(f)

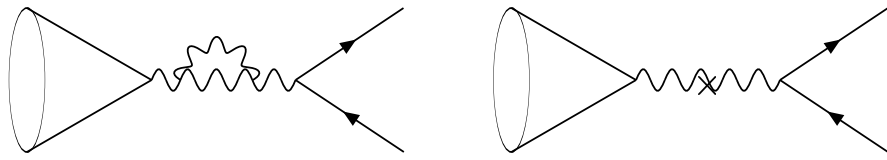
FIG. 3. 2. Self-energy and vertex diagrams for $B_c \rightarrow \ell\nu$.

(g)

(h)

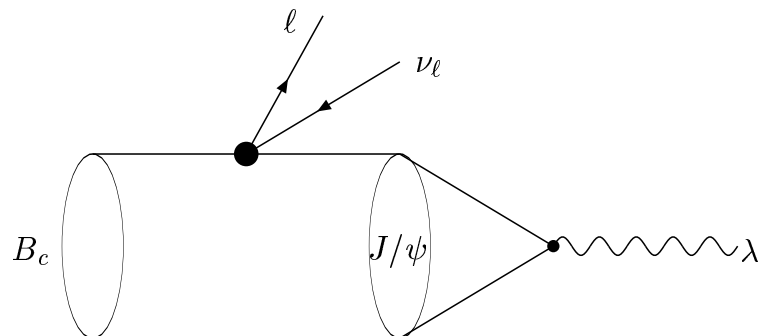
(i)

FIG. 3. 3. Vertex diagrams for $B_c \rightarrow \ell\nu$.

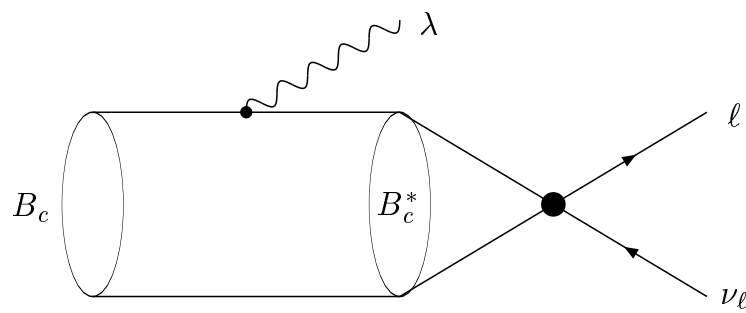


(j)

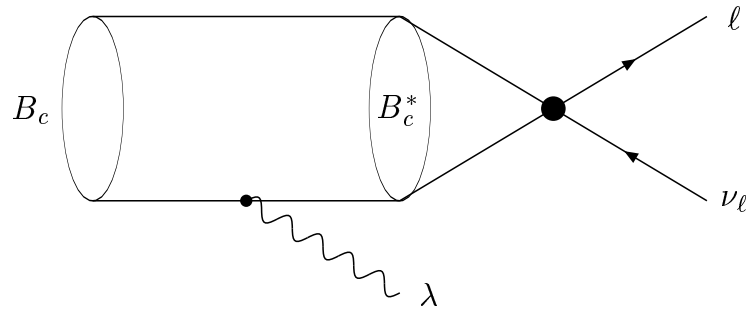
FIG. 3. 4. Self-energy diagrams for $B_c \rightarrow \ell\nu$.



(a)



(b)



(c)

FIG. 4. Diagrams: (a) J/ψ as an intermediate state; (b) and (c) B_c^* as an intermediate state.

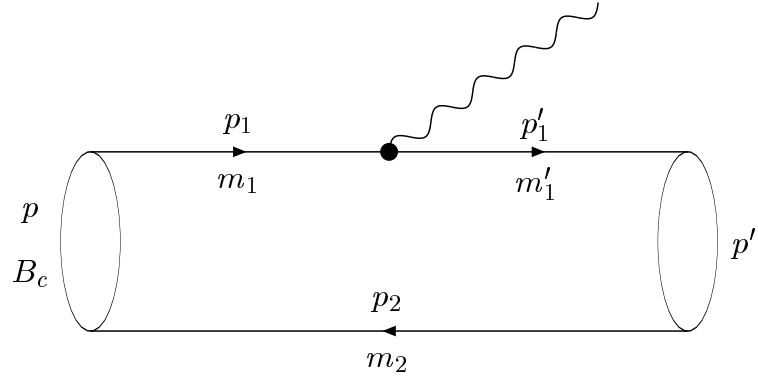


FIG. 5. A Feynman diagram corresponding to the relevant weak or electromagnetic current sandwiched by the B_c meson and a suitable single-particle state.

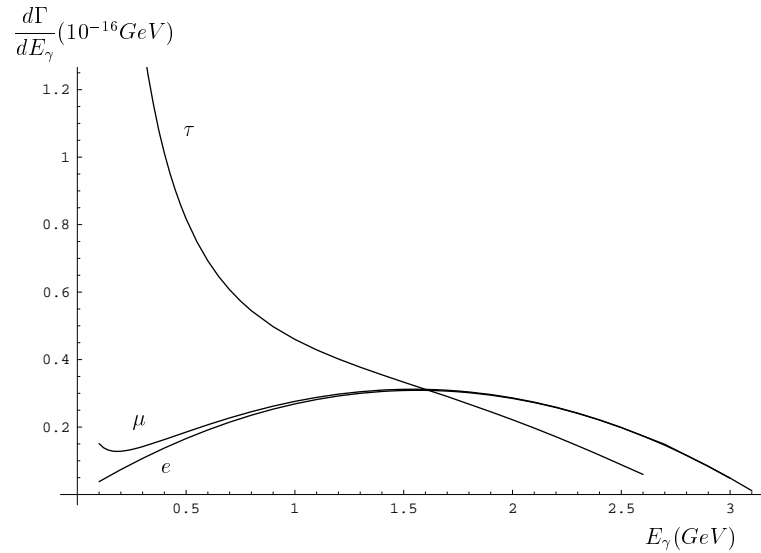


FIG. 6. Photon energy spectra of radiative decays $B_c \rightarrow \ell \nu_\ell \gamma$ ($\ell = e, \mu, \tau$).